

# Photofragmentation of *M*-State Polarized Molecules: Comparison of Quantum and Semiclassical Treatments

Leonard C. Pipes, Nathan Brandstater, Christopher D. Fuglesang, and Delroy Baugh\*<sup>†</sup>

Department of Chemistry and Biochemistry, University of California, Los Angeles, California 90095-1569

Received: April 2, 1997; In Final Form: June 10, 1997<sup>⊗</sup>

A beam of rovibrational energy level selected and magnetic state polarized ( $\tilde{X}^1A_1$ ) CD<sub>3</sub>I  $|JKM\rangle \equiv |111\rangle$  was photodissociated at 266 nm. State-selective detection of the photoproducts allowed determination of elements of the *transition dipole matrix* or **T** matrix. We present here the methodology involved in the extraction of the **T** matrix elements from such quantum state-to-quantum state experiments and furthermore compare the results to cases where quantum and semiclassical descriptions are expected to be most accurate. A brief description of the effects of nuclear-spin depolarization on the accurate determination of the **T** matrix elements is also included. After depolarization is taken into account, the magnitudes of the **T** matrix elements for the  $R(\Delta J = 1)$  and  $Q(\Delta J = 0)$  product waves were 6.4 and 6.9, respectively. The relative phase between these waves was  $\pm 11^\circ$ , which is due purely to the structure of the excited state potential surface. These **T** matrix values give a  $\beta = 1.94$  for the photodissociation of CD<sub>3</sub>I at 266 nm.

## Introduction

Over the past 15 years, photodissociative “half-collision” reactions of small molecules have ascended to a position of prominence in the study of molecular reaction dynamics. Pioneering experimental studies of these relatively simple reactions have yielded a wealth of insight on the nature of molecular motion during the breaking and, consequently, the formation of chemical bonds.<sup>1</sup> The ultimate objective of these molecular photofragmentation studies is the complete description of an elementary chemical reaction in terms of the theory of quantum mechanical scattering. Such studies would provide the most detailed information that is obtainable from a chemical reaction. However, these so-called “complete” experiments require energy level selected and magnetic state (*M*-state) polarized reagents (photon and parent molecules) and the determination of the energy level populations and the *M*-state polarization of the products. In other words, these “complete” experiments measure the detailed differential photofragmentation cross-sections (DDPCS) and consequently the elements of the transition dipole or **T** matrix. The first such experiments were recently reported by Pipes *et al.* who measured the **T** matrix elements for the photodissociation of *M*-state polarized CD<sub>3</sub>I to *M*-state polarized CD<sub>3</sub> radicals and excited I(<sup>2</sup>P<sub>1/2</sub>).<sup>2</sup>

Methyl iodide has become a particularly well-studied molecule both theoretically<sup>3–6</sup> and experimentally<sup>7–20</sup> primarily because of the apparent simplicity with which it can be theoretically modeled. Moreover, since methyl iodide is a symmetric top with a large permanent dipole moment, it can be easily state selected using electrostatic hexapole fields. The early work of Bernstein and co-workers<sup>21</sup> and later work of Stolte *et al.*<sup>22</sup> and Baugh *et al.*<sup>23</sup> has shown that initial state selection of methyl iodide is indeed viable and that rotational states with low quantum numbers (*e.g.*  $J_i = 1, 2$ ) can be produced with >98% purity. As a consequence a whole new level of experimental detail opens up whereby the amplitudes and phases of the **T** matrix elements, *i.e.* the probabilities and coherences for producing reaction products, can now be measured. Such measurements free theorists of the need to

consider the geometric  $(2J + 1)$  degeneracies of the initial reagent and final products states. Theorists can now directly compare the amplitudes and phases of the **T** matrix elements determined in the body-fixed frame to those obtained from these truly state-to-state experiments.

Here we will elaborate on the method that was used to determine the **T** matrix elements in ref 2 and in the process illustrate the differences between the scattering at low rotational quantum numbers where quantum effects predominate and at higher quantum numbers—and/or when the initial parent states are highly averaged—where semiclassical treatments become more accurate.

## Formalism

For the sake of simplicity we will only treat the case of helicity conservation between the parent CD<sub>3</sub>I and the fragment CD<sub>3</sub> radical. This seems reasonable in light of the fact that, to a first approximation,<sup>24</sup> the C<sub>3</sub> symmetry axis is preserved during excitation between the ground potential energy surface (PES)  $\tilde{X}^1(A_1)$  and the excited A(<sup>3</sup>Q<sub>0</sub>) adiabatic surface, at least in the Franck–Condon region. It follows that if the fragments are ejected parallel to the initial C–I bond direction, then parallel excitation should lead to the conservation of the helicity quantum number  $K$ .<sup>3–10</sup> In any event, since both CD<sub>3</sub>I and CD<sub>3</sub> are symmetric tops, the formalism developed by Balint-Kurti and Shapiro<sup>25</sup> and later by Seideman<sup>26</sup> can be readily used to describe the scattering amplitude,  $f(\mathbf{k}; NK_N M_N | J_i K_i M_i)$ , for the photodissociation of state-selected CD<sub>3</sub>I.

$$f(\mathbf{k}; NK_N M_N | J_i K_i M_i) = (-1)^{N+M_N} \sum_{JMKps} (-1)^K \hat{J} / (4\pi)^{1/2} D_{KM}^J(\mathbf{k}) D_{-K-M_N}^N(\mathbf{k}) \epsilon_p (3\pi/8)^{1/2} \hat{J}_i (1 + \delta_{s0})^{-1/2} \begin{pmatrix} J & 1 & J_i \\ -M & p & M_i \end{pmatrix} (-1)^{K+M} \left\{ \begin{pmatrix} J & 1 & J_i \\ -K & s & K_i \end{pmatrix} + (-1)^s \begin{pmatrix} J & 1 & J_i \\ -K & -s & K_i \end{pmatrix} \right\} t(E; JNK | E_i J_i K_i) \quad (1)$$

Here  $\epsilon_p$  is the spherical component of the electric field vector of the photolysis laser,  $\hat{J} = (2J + 1)^{1/2}$ ,  $J$ ,  $K$ , and  $M$  are the quantum numbers for the total angular momentum of the coupled molecule–photon system, its projection along the C<sub>3</sub>

<sup>†</sup> This paper is dedicated to the memory of Richard B. Bernstein.

<sup>⊗</sup> Abstract published in *Advance ACS Abstracts*, September 15, 1997.

molecular axis (body-fixed *z*-axis), and its projection on the laboratory *Z*-axis, respectively, *s* characterizes the spherical components of the transition dipole moment vector field (*i.e.*  $s = 0$  for a purely parallel transition),  $D_{KM}^J(\mathbf{k})$  are Wigner rotation matrices,  $\begin{pmatrix} J & 1 & J \\ -K & s & K_i \end{pmatrix}$  is a three-*j* symbol, and *N* is the rotational angular momentum of the photofragment (CD<sub>3</sub>) less electron spin. The terms  $t(E;JNK_i|E_iJ_iK_i)$  are the **T** matrix elements and are equal to the integral of the reduced *transition dipole operator* and the scattered and initial state wavefunctions over all body-fixed coordinates. Note that  $K_N = K_i$  hereafter (helicity conservation).

The products  $f(\mathbf{k};NK_iM_N|J_iK_iM_i) f(\mathbf{k};NK_iM'_N|J_iK_iM_i)^*$  are the angle-dependent density matrix elements  $\rho_{M_NM'_N}(\mathbf{k};NK_i)$  for the CD<sub>3</sub> fragment resulting from the photofragmentation of the CD<sub>3</sub>I parent in a single  $|J_iK_iM_i\rangle$  quantum state. When the magnetic quantum numbers  $M_N$  and  $M'_N$  are different, these off-diagonal elements of the fragment density matrix  $\rho_{M_NM'_N}(\mathbf{k};NK_i)$  describe the coherence between the CD<sub>3</sub> *M*-states. The diagonal elements,  $M_N = M'_N$ , are the *detailed differential photofragmentation cross-sections* (DDPCS),  $\sigma(\mathbf{k};NK_iM_N|J_iK_iM_i)$ , which do not include *M*-state coherence:

$$\begin{aligned} \sigma(\mathbf{k};NK_iM_N|J_iK_iM_i) &= (4\pi^2\omega/c)|f|^2 = (3\pi^2\omega/4c) \sum_{J'JM'p'p} \\ &(-1)^{M'+M} \hat{J}^2 \hat{J}'^2 \hat{J}_i^2 D_{K_iM}^J(\mathbf{k}) D_{K_iM'}^{(J^*J')}(\mathbf{k}) D_{-K_i-M_N}^N(\mathbf{k}) D_{-K_i-M_N}^{(N)*}(\mathbf{k}) \\ &(\mathbf{k}) \epsilon_p \epsilon_{p'}^* \begin{pmatrix} J' & 1 & J_i \\ -M & p' & M_i \end{pmatrix} \begin{pmatrix} J & 1 & J_i \\ -M & p & M_i \end{pmatrix} \times \\ &\begin{pmatrix} J' & 1 & J_i \\ -K_i & 0 & K_i \end{pmatrix} \begin{pmatrix} J & 1 & J_i \\ -K_i & 0 & K_i \end{pmatrix} t(E;JNK_i|E_iJ_iK_i) t^*(E;J'NK_i|E_iJ_iK_i) \end{aligned} \quad (2)$$

It is more convenient in our case to describe the system in terms of product state moments, or statistical tensors, since laser-based experimental detection techniques are in general directly sensitive to them.

$$A_q^k(NK_i) = \sum_{M'_NM_N} (-1)^{N-M_N} \hat{N} \begin{pmatrix} N & N & k \\ M_N & M'_N & q \end{pmatrix} \sigma_{M'_NM_N}(\mathbf{k};NK_i|J_iK_i) \quad (3)$$

where  $\sigma_{M'_NM_N}$  is the DDPCS averaged over  $M_i$ . These  $A_q^k$  are statistical tensors of rank *k* and component *q* and are in effect the irreducible components of the product CD<sub>3</sub> density matrix.  $A_q^k$  of odd ranks describe the orientation of the product *N* in the laboratory frame, while  $A_q^k$  of even ranks describe the alignment. Experimental measurement of a sufficient number of final product moments to allow simultaneous solution for the **T** matrix elements (magnitudes *and* phases) is the crux of our method. By insertion of eq 2 into eq 3, a new equation can be written relating each product moment to the transition dipole elements and the moments representing the photolysis photon and the initial parent state.<sup>27</sup> The course at this point becomes divided. Either the experimentalist can determine all of the possible product state moments as a function of recoil direction (*i.e.* determine the state-specific angular distribution and deconvolute any and all vector correlations)<sup>28</sup> or he/she can determine product statistical tensors integrated over all angles. However, the former technique is notoriously difficult and has yet to be fully realized in practice, while the latter technique requires initial *M*-state polarization in order for the system to *exhibit* a sufficient number of state moments to solve directly for the **T** matrix elements. There are several well-known techniques for producing initial state polarization (*e.g.* hexapole focusing and optical pumping)<sup>23,29,30</sup> which could be used for the purpose of

determining **T** matrix elements in this manner. If the angle integrated product statistical tensors, herein referred to as  $\langle A_q^k \rangle$ , are determined, the description of these moments in terms of the **T** matrix elements can be reduced to eq 4.

$$\begin{aligned} \langle A_q^k \rangle &= \sum_{JJ'} 3\pi^2\omega/c \hat{J} \hat{J}' \hat{J}_i^2 (-1)^{N+J'+q} T_q^k(J'J;K_i) \\ &t(E;JNK_i|E_iJ_iK_i) t^*(E;J'NK_i|E_iJ_iK_i) \begin{pmatrix} J & J & k \\ K_i & K_i & 0 \end{pmatrix} \begin{pmatrix} N & N & k \\ -K_i & K_i & 0 \end{pmatrix} \\ &\begin{pmatrix} J' & 1 & J_i \\ -K_i & 0 & K_i \end{pmatrix} \begin{pmatrix} J & 1 & J_i \\ -K_i & 0 & K_i \end{pmatrix} \end{aligned} \quad (4)$$

Here the symbols are as defined above, *J* and *J'* are the possible total angular momenta of the coupled photon molecule system ( $J, J' = J_i, J_i \pm 1$ ), and  $T_q^k(J'J;K_i)$  are the statistical tensors describing the moments of the coupled photolysis-photon/parent-molecule system.<sup>2</sup>

The **T** matrix element description is more detailed than the anisotropy parameter or “ $\beta$ -parameter” description of a photodissociation process because the  $\beta$ -parameter is arrived at by summing eq 2 over all initial and final product *M*-states. This is necessary in most molecular beam experiments that do not incorporate initial quantum state selection, since even very cold beams contain several rotational and magnetic quantum states. These sums are usually buried in the  $\beta$ -parameter, and significant information about the photofragmentation dynamics is therefore lost in this averaging process—thus making determination of the **T** matrix elements directly from measurements of the  $\beta$ -parameter extremely difficult.

## Experimental Section

Only a brief description of the experimental setup is given here; a more complete description can be found elsewhere.<sup>24</sup> A gas pulse of CD<sub>3</sub>I seeded in Xe (~5–10%) was skimmed and chopped before entering an electrostatic hexapole state-selector. The state-selected molecular beam exited the hexapole field about 3 m downstream from the source nozzle and entered a uniform electric dipole field that adiabatically oriented the permanent molecular dipoles in the laboratory frame and also served to define the laboratory *Z*-axis. Consequently the CD<sub>3</sub>I angular momentum vector (**J**) was aligned by the dipole field along the laboratory *Z*-axis. The state-selected molecular beam then entered the photodissociation/detection chamber ( $P = 10^{-9}$  Torr) where it was crossed at 90° by collinear, counterpropagating, linearly polarized photolysis and probe laser beams. The photolysis laser (266.2 nm, 3 mJ/pulse) was the quadrupled output of an Nd:YAG, and its polarization was kept parallel to the *Z*-axis to maintain the cylindrical symmetry of the experimental setup. The probe laser (3 mJ/pulse) was a dye laser tuned to the rotational branches of the CD<sub>3</sub> 0<sub>0</sub> vibronic band of the  $3p^2A_2'' \leftarrow 2p^2A_2''$  electronic transition (~333.8 nm). The polarization of the probe laser was controlled by a  $\lambda/2$  plate. Delayed 10–20 ns relative to the photolysis laser, the probe laser ionized the methyl photofragments via (2 + 1) REMPI and the resultant ions were collected by a Wiley-McLaren time-of-flight (TOF) spectrometer oriented parallel to the positive *Z*-axis in the laboratory frame. In some experiments the probe laser was tuned to ionize the product iodine atom in its excited spin-orbit state (<sup>2</sup>P<sub>1/2</sub>) at ~343.3 nm

## Results and Discussion

The **T** matrix elements have been determined experimentally for an initial CD<sub>3</sub>I state  $|J_iK_iM_i\rangle = |11-1\rangle$  or  $|1-11\rangle$ , hereafter referred to as the  $|111\rangle$  state, producing CD<sub>3</sub> photofragments in states  $|NK_iM\rangle = |111\rangle$  and  $|211\rangle$ , using a linearly polarized

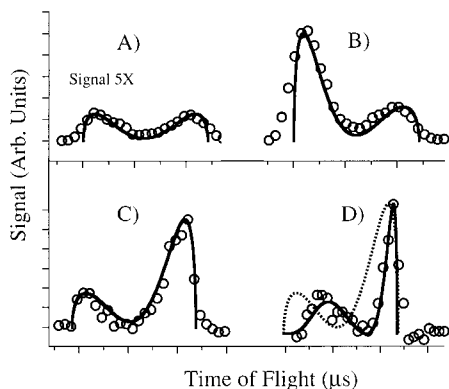


**Figure 1.** (A) Experimental TOF spectrum ( $\times 5$ ) of non-state-selected iodine ( $-\circ-$ ) with simulated TOF spectrum ( $-$ ) using the semiclassical expression of eq 5 with  $|\psi(\theta)_{J,K_i,M_i}|^2 = 1$ . (B) Experimental TOF spectrum state-selected iodine ( $-\circ-$ ) with simulated TOF spectrum ( $-$ ) using the semiclassical expression of eq 5 with  $|\psi(\theta)_{J,K_i,M_i}|^2 = |\psi(\theta)_{111}|^2$ . (C) Experimental TOF spectrum state-selected methyl iodide ( $-\circ-$ ) on Q-branch transition with simulated TOF spectrum ( $-$ ) using the semiclassical expression of eq 5 with  $|\psi(\theta)_{J,K_i,M_i}|^2 = |\psi(\theta)_{111}|^2$ . (D) Experimental TOF spectrum state-selected methyl iodide ( $-\circ-$ ) on P(2)-branch transition with simulated TOF spectrum ( $-$ ) using the semiclassical expression of eq 5 with  $|\psi(\theta)_{J,K_i,M_i}|^2 = |\psi(\theta)_{111}|^2$  and with simulated ( $- -$ ) TOF spectrum using  $t(J=1) = 6.4$ ,  $t(J=2) = 6.9$  and a phase difference of  $79^\circ$ .

photolysis laser with its electric vector held parallel to the laboratory Z-axis (thereby making  $\Delta M = 0$  for the photolysis excitation step).<sup>34,35</sup> The  $M$ -state polarization of the  $\text{CD}_3$  fragment, *i.e.* the  $\langle A_q^k \rangle$  moments, were determined from angle integrated spectra as demonstrated in ref 2. For these experiments no odd-ranked moments could be measured since the  $\text{CD}_3\text{I}$   $\mathbf{J}$  vector was aligned and not oriented and only linearly polarized photolysis and probe photons were used to produce and detect the  $\text{CD}_3$  fragment. Due to the cylindrical symmetry of the experimental setup, only components with  $q = 0$  could be nonzero. From eq 3, this also means that only the diagonal elements of the fragment density matrix will be nonzero. These limitations in the allowed ranks and components greatly simplify the analysis of the experimental data. However, once the  $\mathbf{T}$  matrix elements have been measured experimentally, it is relatively straightforward to go back to the theory to calculate the expected moments and angular distributions for any case of interest at this photolysis wavelength.

What is of further interest is the dependence of angular distributions on the methyl radical rotational angular momentum quantum number,  $N$ . In general full angular distributions are not observable experimentally since most detection schemes employ a specific number  $n$  of resonant photons  $\{i.e. (n + m)$  REMPI, *etc.*  $\}$  and are therefore intrinsically only sensitive to statistical tensors ranks  $k$  up to  $2n$  due to the spin of the photon,  $S_{\text{photon}} = 1$ . However, it is straightforward to take into consideration these effects, the observed angular distributions in the form of time-of flight (TOF) profiles (Figure 1), which represent the projection of the three-dimensional photoproduct angular distribution on the laboratory Z-axis. Figure 1 shows both iodine (Figure 1a,b) and methyl (Figure 1c,d) TOF spectra, all originating from an initial  $\text{CD}_3\text{I}$   $|111\rangle$  state. Superimposed upon these experimental data are simulated TOF spectra utilizing a semiclassical approximation (eq 5)<sup>27</sup> with a  $\beta = 1.8$  as has been previously reported.<sup>34,35</sup>

In our case, the cylindrical symmetry of the experiment reduces the TOF profiles to only two-dimensional projections. For the TOF spectra of methyl photoproducts in a single  $|JK\rangle$  level, the speed distribution is effectively a  $\delta$ -function in the center-of-mass frame, and therefore the shape of the spectrum

is solely dependent on the angular distribution of photoproduct recoil velocity vectors. However, this is not true for TOF spectra of the iodine atom photoproduct since they represent a sum over *all* methyl photofragment states (rotational and vibrational) that correlate with the (detected) product iodine atoms in the excited spin-orbit state. These definitely differ in recoil speeds and undoubtedly differ in angular distributions (the extent to which they differ depends upon the degree of rotational excitation of the methyl fragment). Because the iodine TOF spectrum (Figure 1a,b) represents a sum over all methyl photofragment states, we expect it to be dominated by sums over many  $\text{CD}_3$  rotational angular momenta with  $N > 2$ , and should in turn be adequately described by semiclassical treatments as described by eq 5.<sup>31,32</sup>

$$I(\theta) = |\psi(\theta)_{J,K_i,M_i}|^2 [1 + \beta P_2(\cos \theta)] \quad (5)$$

This is due to the fact that quantum interference effects for any given state-to-state angular distribution are expected to become increasingly oscillatory for larger and larger final rotational angular momenta, therefore washing out any such effects from the TOF spectrum. The most obvious difference between the iodine and methyl TOF spectra are the relative peak shapes which merely reflect that the iodine atom is oriented opposite to the direction of the methyl moiety in the state-selected  $\text{CD}_3\text{I}$  beam. Note how well the iodine atom TOF's of Figure 1a,b match the semiclassical simulation. This agreement between experimental TOF profiles and the semiclassical angular distribution was also observed if the methyl radical was detected on a Q-branch band head—in its lowest vibrational level ( $v'' = 0$ )—where the overlap of several rotational transitions precludes excitation of a single rotational level, Figure 1c. Note that unlike the I-atom TOF profiles, the TOF profile of the  $v'' = 0$  methyl radicals correspond to a well-defined speed (the average rotational energy is only  $70 \text{ cm}^{-1}$ )<sup>24</sup> and is therefore much sharper at the wings of the TOF profile. Since the Q-branch transition corresponds to methyl radicals in several rotational levels, up to  $N = 9$ , this agreement is not surprising. On the other hand, the poor fit of eq 5 to the methyl TOF spectrum when detection is via a P-branch transition which corresponds to  $N = 2$  and  $K_N = 1$  and from ref 2,  $M = 1$ , points to the inadequacy of the semiclassical description to an inherently quantum mechanical system where the angular momentum quantum numbers of both parent and products are small, *i.e.*  $J_i$  and  $N \leq 2$ . Since the  $\text{CD}_3$  radical was detected via a two-photon resonance and the experimental geometry was cylindrically symmetric, these TOF spectra are sensitive to all possible moments ( $A_0^0$ ,  $A_0^2$ , and  $A_0^4$ ) of the  $\text{CD}_3$  radical and are in a sense complete experiments. The only observable not determined by these experiments is the *absolute* phase of the  $\mathbf{T}$  matrix elements for excitation of  $\text{CD}_3\text{I}$  in energy level  $|J_i K_i\rangle = |11\rangle$  to  $\text{CD}_3$  ( $v'' = 0$ ) in rotational energy levels  $N = 2$  with  $K_N = 1$ .<sup>2</sup>

It is clear that the accurate determination of the  $\mathbf{T}$  matrix elements using eq 4 requires knowledge of the initial parent  $M$ -state and the photolysis laser electric vector polarizations (or their corresponding statistical tensor moments). The direct product of these moments gives the coupled parent/photon or initial-state moment  $T_q^k(JJ;K_i)$  used in eq 4.<sup>27</sup> Direct experimental determination of the parent  $M$ -state distributions, for a hexapole focused molecule, has to our knowledge only been obtained for one system,  $\text{ND}_3$ .<sup>23</sup> These measurements were performed using resonance enhanced multiphoton ionization (REMPI) of  $\text{ND}_3$ . However, due to the predissociative nature of the  $\text{CD}_3\text{I}$  excited states, such direct measurements of the parent  $\text{CD}_3\text{I}$  polarization are not possible and one must resort to more

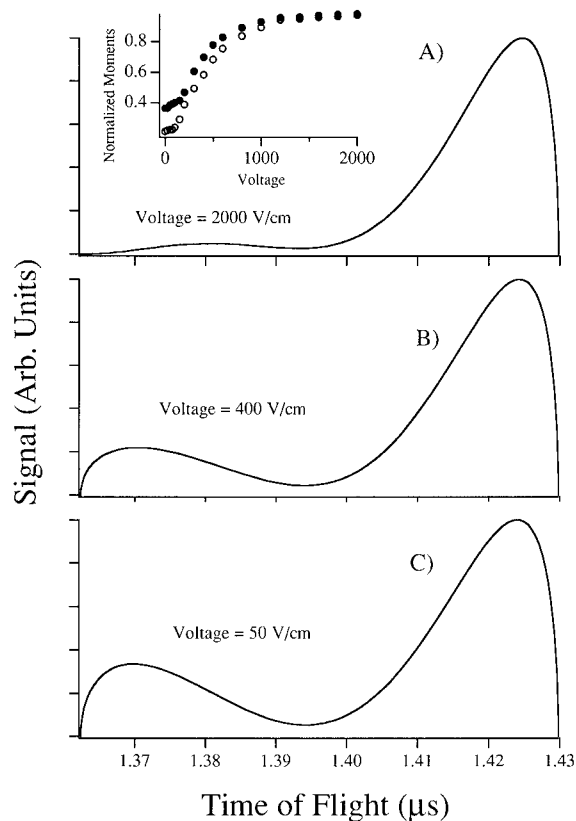


**Figure 2.** Simulated TOF spectra using the semiclassical expression of eq 5 with calculated initial *M*-state depolarization at extraction voltage equal to (A) 50, (B) 400, and (C) 2000 V. Inset: Plot of normalized alignment moments  $A_0^1/A_0^1(\max)$  (●) and  $A_0^2/A_0^2(\max)$  (○) for the  $|11-1\rangle$  or  $|1-11\rangle$  states vs orientation voltage.

indirect methods. We use the photofragmentation method first proposed by Gandhi *et al.*<sup>21</sup> and later used by Mastenbroek *et al.*<sup>36</sup> to show the effect of the orientation field strength on the  $\text{CD}_3\text{I}$  initial *M*-state polarization.

The problem of primary interest is the depolarization of the  $\text{CD}_3\text{I}$   $|J_i K_i M_i\rangle$  state by the nuclear spin (*i.e.* quadrupole coupling of the iodine atom) during its flight through the “weak” dipole orienting field and ion extraction field. At one extreme the  $\text{CD}_3\text{I}$   $|JKM\rangle$  state completely transfers its polarization to nuclear spin polarization, causing the *M*-states to mix substantially, thereby changing the initial state moments of eq 4. This polarization transfer only depends on the ratio of the linear Stark energy (and therefore the instantaneous electric field strength) to the nuclear quadrupole coupling energy. Since the photodissociation process occurs on the femtosecond time scale, it is insensitive to the dynamics of nuclear spin state polarization which occurs on a much slower time scale. The depolarization of the parent  $\text{CD}_3\text{I}$  **J** vector should then only affect the initial laboratory *M*-state distribution and not the photodissociation process occurring in the molecular frame. The relevant question is then the degree to which this depolarization changes the *M*-states of the parent  $\text{CD}_3\text{I}$  under the experimental conditions, namely, the orienting dipole voltage  $\sim 200 \text{ V cm}^{-1}$ . Figure 2, shows a series of simulated methyl TOF spectra calculated using the semiclassical approximation of eq 5, each with a different dipole orientation voltage per centimeter and thus a different degree of depolarization. Inset in Figure 2 is a graph showing the magnitude of the  $A_0^1$  and  $A_0^2$  initial molecular moments (normalized to their limiting values) as a function of the orienting voltage. The procedure used to determine the degree of depolarization due to iodine nuclear quadrupole coupling is straightforward and is expounded upon elsewhere.<sup>37</sup> What is

of immediate interest is the sensitivity of the TOF spectra to the strength of the orienting dipole field and that the effects of depolarization on the methyl photofragment angular distributions and on the integrated moments can be readily accounted for.

The fits to the I-atom and  $\text{CD}_3(v'' = 0)$  TOF spectra shown in Figure 2, using eq 5, all include the effect of depolarization due to the I-atom quadrupole coupling by summing eq 5 over all initial parent  $M_i$ -states weighted by the appropriate probabilities as calculated for the initial state moments in the Figure 2 inset.<sup>32,33</sup> As noted above, for those cases where many  $\text{CD}_3$  rotational states are involved, the semiclassical treatment is satisfactory as is shown by the agreement between the experimental and simulated TOF spectra (Figure 1). These same  $\text{CD}_3\text{I}$  initial state moments can therefore be used in eq 4 to derive the **T** matrix elements as was done in ref 2, where the effect of depolarization was not included. The previous values of the **T** matrix elements for the R-branch and P-branch waves,  $|t(J = 2)| = 1.32$  and  $|t(J = 1)| = 0.5$ , respectively, with a relative phase of  $120^\circ$  can now be updated with the more accurate values which now include the effect of the  $\text{CD}_3\text{I}$  depolarization. The new values for the R-branch and P-branch waves, are  $|t(J = 2)| = 6.4$  and  $|t(J = 1)| = 6.9$ , respectively, with a relative phase of  $\pm 79^\circ$ . As was shown by Zare,<sup>38</sup> this value includes the  $90^\circ$  phase shift due to the centrifugal contribution to the effective excited state potential surface seen by the departing fragment. When this  $90^\circ$  phase shift is removed, one obtains a phase shift between the R- and Q-branch waves of  $11^\circ$ . Note that this is purely a molecular attribute introduced solely by the structure of the excited state potential energy surface at 266.2 nm and is therefore a fundamental property of the molecule. We must note, however, that to be truly useful the dependence of these quantities (**T** matrix elements) on the frequency of the photolysis photon should be determined as well. Finally, using these numbers, a  $\beta = 1.94$  can be calculated.<sup>37,39</sup> The only assumption necessary to obtain this  $\beta$  is that the parent  $\text{CD}_3\text{I}$  is energy-level selected to be in its ground vibrational state ( $v'' = 0$ ) with  $|J_i K_i\rangle = |11\rangle$ . This number is clearly in excellent agreement with the values from non-state-selected experiments.<sup>34,35</sup> We explain the deviation from the limiting value of  $\beta = 2.0$  by the finite rotation time of the molecule before the fragments become free of each other, *i.e.* when the potential energy between the fragments ceases to affect their relative motion.<sup>39</sup>

## Summary and Conclusion

It was previously shown that photodissociation studies which incorporate production of reagents in single rovibronic and magnetic states with state-selective detection of the photoproducts allow the experimental determination of the *transition dipole matrix*. In this paper we have described the method for extracting these **T** matrix elements from experimental data and used this information to compare the applicability of a quantum and a semiclassical treatment of photodissociation processes. Although the semiclassical treatment well-represents the cases where several rotational states and/or states of high rotational angular momenta are involved, it does not adequately describe the results for single quantum states at low values of rotational angular momenta. This we believe points to the importance of interference effects in the “quantum” regime.

Also discussed in this paper is the influence of depolarization of the initial parent **J** vector on the amount of information that can be extracted from “state-to-state” photoreactions. Despite significant interaction between the nuclear quadrupole moment of iodine and the angular momentum vector of the parent  $\text{CD}_3\text{I}$ , the effect upon the angular distribution and the product moments

is readily accounted for. Here we have included the effect of depolarization and reported the new more accurate values for the **T** matrix elements for excitation of  $v'' = 0$  CD<sub>3</sub>I in the rotational energy level  $|J_i K_i\rangle = |11\rangle$  to CD<sub>3</sub>( $v'' = 0$ ) in rotational energy levels  $N = 2$  with  $K_N = 1$  as well as the corresponding  $\beta$  value. We believe that this is the first report of a  $\beta$  value derived from experimentally measured transition amplitudes for a chemical reaction.

**Acknowledgment.** We are extremely grateful to the National Science Foundation (NSF) for the support to do this work through the Young Investigator program, Grant No. DMR-9257433, and through Grant No. CHE-9414931. Additional support was provided by the UCLA Academic Senate and the UCLA Office of the Dean of Physical Sciences. We also wish to acknowledge the support of the Ford Motor Co. Fund and the Hewlett-Packard Co.

## References and Notes

- (1) Schinke, R. *Photodissociation Dynamics*; Cambridge University Press: Cambridge, U.K., 1993.
- (2) Pipes, L. C.; Kim, D. Y.; Brandstater, N.; Fuglesang, C. D.; Baugh, D. *Chem. Phys. Lett.* **1995**, *247*, 564.
- (3) Shapiro, M. *J. Phys. Chem.* **1986**, *90*, 3644.
- (4) Amatasu, Y.; Morokuma, K.; Yabushita, S. *J. Chem. Phys.* **1991**, *94*, 4858.
- (5) Guo, H. *J. Chem. Phys.* **1992**, *96*, 6629.
- (6) Hammerlich, A. D.; Manthe, U.; Kosloff, R.; Meyer, H.-D.; Cederbaum, L. S. *J. Chem. Phys.* **1994**, *101*, 5623.
- (7) Chandler, D. W.; Janssen, M. H. M.; Stolte, S.; Strickland, R. N.; Thoman, J. W., Jr.; Parker, D. H. *J. Phys. Chem.* **1990**, *94*, 4839.
- (8) Janssen, M. H. M.; Parker, D. H.; Sitz, G. O.; Stolte, S.; Chandler, D. W. *J. Phys. Chem.* **1991**, *95*, 8007.
- (9) Loo, R. O.; Haerri, H.-P.; Hall G. E.; Houston, P. L. *J. Chem. Phys.* **1989**, *90*, 4222.
- (10) Zahedi, M.; Harrison J. A.; Nibler, J. W. *J. Chem. Phys.* **1994**, *100*, 4043.
- (11) Powis, I.; Black, J. F. *J. Phys. Chem.* **1989**, *93*, 2461.
- (12) Gedanken, A.; Rowe, M. D. *Chem. Phys. Lett.* **1975**, *34*, 39.
- (13) Hertz R. A.; Syage, J. A. *J. Chem. Phys.* **1994**, *100*, 9265.
- (14) Sparks, R. K.; Shobatake, K.; Carlson L. R.; Lee, Y. T. *J. Chem. Phys.* **1981**, *75*, 3838.
- (15) Van Veen, G. N. A.; Baller, T.; DeVries, A. E. *Chem. Phys.* **1985**, *97*, 179.
- (16) Person, M. D.; Kash P. W.; Butler, L. J. *J. Chem. Phys.* **1991**, *94*, 2557.
- (17) Baughcum, S. L.; Leone, S. R. *J. Chem. Phys.* **1980**, *72*, 6531.
- (18) Wang, P. G.; Ziegler, L. D. *J. Phys. Chem.* **1993**, *97*, 3139.
- (19) Butler, L. J.; Neumark, D. M. *J. Phys. Chem.* **1996**, *100*, 12801.
- (20) Johnson, B. R.; Kinsey, J. L. *J. Phys. Chem.* **1996**, *100*, 18937.
- (21) Gandhi, S. R.; Curtiss, T. J.; Bernstein, R. B. *Phys. Rev. Lett.* **1987**, *59*, 2951.
- (22) Bulthuis, J.; Millan, J. B.; Janssen, M. H. M.; Stolte, S. *J. Chem. Phys.* **1991**, *94*, 7181.
- (23) Baugh, D. A.; Kim, D. Y.; Cho, V. A.; Pipes, L. C.; Petteway J. C.; Fuglesang, C. D. *Chem. Phys. Lett.* **1994**, *219*, 207.
- (24) Kim, D. Y.; Brandstater, N.; Pipes, L.; Garner, T.; Baugh, D. J. *J. Phys. Chem.* **1995**, *99*, 4364.
- (25) Balint-Kurti, G. G.; Shapiro, M. *Chem. Phys.* **1981**, *61*, 137.
- (26) Seideman, T. *J. Chem. Phys.* **1995**, *102*, 6487.
- (27) Fuglesang, C. D.; Baugh, D. A.; Pipes, L. C. *J. Chem. Phys.* **1996**, *105*, 9796.
- (28) Siebbeles, L. D. A.; Glass-Maujean, M.; Vasyutinskii, O. S.; Beswick, J. A.; Roncero, O. *J. Chem. Phys.* **1994**, *100*, 3610.
- (29) Bergman, K. In *Atomic and Molecular Beam Methods*; Scoles, G., Ed.; Oxford University Press: Oxford, U.K., 1988; p 293.
- (30) Allendorf, S. W.; Leahy, D. J.; Jacobs, D. C.; Zare, R. N. *J. Chem. Phys.* **1989**, *91*, 2216.
- (31) Zare, R. N. *Chem. Phys. Lett.* **1989**, *156*, 1.
- (32) Choi, S. E.; Bernstein, R. B. *J. Chem. Phys.* **1986**, *85*, 150.
- (33) Bulthuis, J.; Stolte, S. *J. Phys. Chem.* **1991**, *95*, 8180.
- (34) Dzvonik, M.; Yang, S.; Bersohn, R.; *J. Chem. Phys.* **1974**, *61*, 4409.
- (35) Loo, R. O.; Hall, G. E.; Haerri, H.-P.; Houston, P. L. *J. Phys. Chem.* **1988**, *92*, 5.
- (36) Mastenbroek, J. W.; Nanta, B. K.; Jennsen, M. H. N.; Stolte, S. *SPIE Proc. V* **1995**, *2548*, 9.
- (37) Fuglesang, C. D. Ph.D. Thesis, University of California, Los Angeles, 1997.
- (38) Zare, R. N. *Mol. Photochem.* **1972**, *4*, 1.
- (39) Pipes, L. C.; Torres, E. A.; Baugh, D. A. Manuscript in preparation.